Determination of the Poisson ratio of (001) and (111) oriented thin films of In_2O_3 by synchrotron-based x-ray diffraction

K. H. L. Zhang, A. Regoutz, R. G. Palgrave,* D. J. Payne,† and R. G. Egdell‡
Department of Chemistry, Inorganic Chemistry Laboratory, University of Oxford, South Parks Road, Oxford OX1 3QR, United Kingdom

A. Walsh
Centre for Sustainable Chemical Technologies and Department of Chemistry, University of Bath, Claverton Down, Bath BA2 7AY, United Kingdom

S. P. Collins
Diamond Light Source, Harwell Science and Innovation Campus, Didcot, Oxfordshire OX11 0DE, United Kingdom

D. Wermeille
XMaS CRG Beamline, European Synchrotron Radiation Facility, 38043 Grenoble Cedex 9, France and Department of Physics, University of Liverpool, Liverpool L69 7ZE, United Kingdom

R. A. Cowley
Clarendon Laboratory, Department of Physics, University of Oxford, Parks Road, Oxford OX1 3PU, United Kingdom
(Received 25 October 2011; published 1 December 2011)

The Poisson ratio ν of In_2O_3 has been determined by measurement of the covariation of in-plane and out-of-plane lattice parameters of strained thin films grown epitaxially on (111) and (001) oriented cubic Y-stabilized ZrO_2 substrates. The experimental results are in good agreement with values for ν calculated using atomistic simulation procedures.

DOI: 10.1103/PhysRevB.84.233301 PACS number(s): 68.60.Bs, 61.05.cf, 81.15.Hi

Transparent conducting oxides (TCOs) combine the properties of optical transparency in the visible region with a high electrical conductivity, and they have widespread application as window electrodes in photovoltaic devices, liquid crystal displays, and organic light-emitting diodes.[1,2] Indium oxide (In_2O_3) is a prototypical TCO, which is amenable to degenerate n-type doping with Sn to give so-called indium tin oxide (ITO). In spite of the undoubted technological importance of ITO, many of the basic physical properties of In_2O_3 itself have proved to be controversial, including the nature and magnitude of the band gap. Recently, it has been established that In_2O_3 has a direct but forbidden band gap of $\sim$2.9 eV,[3] almost 1 eV lower than the widely quoted value of 3.75 eV, which marks the onset of allowed optical absorption.[4] Moreover it has been shown that growth of strained In_2O_3 single-crystal thin films on cubic Y-stabilized ZrO_2 (YSZ) substrates leads to a reduction in the value of the band gap.[5] The YSZ substrate places the film under tensile strain owing to a -1.7% mismatch in lattice parameters, and the reduction of the gap arises from in-plane expansion of the In_2O_3, which in turn reduces the bonding-antibonding interactions between O $2p$ and In $5s/5p$ states. The effects of in-plane tensile strain are partially compensated by a reduction in interatomic separations in the orthogonal longitudinal direction through the Poisson effect. The magnitude of this contraction is determined by the Poisson ratio (ν) for In_2O_3, and the magnitude of ν is clearly the critical parameter in tuning the band gap by elastic strain. However, there have been few attempts to determine the Poisson ratio of In_2O_3 experimentally.

In_2O_3 adopts a body-centered cubic bixbyite structure, with space group $Ia\bar{3}$ and lattice parameter $a_e = 10.1170$ Å.[6] The structure is based on a $(2 \times 2 \times 2)$ superstructure of fluorite with ordered removal of oxygen ions from $\frac{1}{4}$ of the oxygen lattice sites. The face-centered cubic fluorite structure of Y-stabilized ZrO_2 (YSZ) belongs to the space group $Fm\bar{3}m$. The cubic lattice parameter of YSZ varies with Y doping level and is measured to be $a_s = 5.1447$ Å at the 17% Y doping level of substrates used in the current work: The subscripts in a_s and a_e denote the substrate and the epilayer, respectively. Thus, there is a mismatch m of -1.68% between $2a_s$ for YSZ (10.2894 Å) and a_e for In_2O_3, where m is defined by:

$$m = \frac{a_e - 2a_s}{2a_s} \times 100\%.$$

It is becoming clear that (111) oriented Y-stabilized ZrO_2 is the most promising substrate for hetero-epitaxial growth of continuous and highly oriented In_2O_3 thin films,[7–9] owing to the fact that (111) surfaces of In_2O_3 have the lowest energy amongst the low-index surfaces.[10] By contrast, growth on (001) surfaces leads under many conditions to films with an island-like morphology.[11–13] The island growth mode is driven by development of low-energy $\{111\}$ side facets. For sufficiently large islands, mismatch between the substrate and the epilayer is compensated in part by tilting of the islands: This leads to splitting of spots in reciprocal space maps.[14] However, for sufficiently small islands, it is anticipated that mismatch will be accommodated by strain rather than tilt.[15] In the current Brief Report, we present a study by high-resolution x-ray diffraction of strained (but not tilted) epitaxial thin films of In_2O_3 grown on (111) and (001) oriented cubic Y-stabilized ZrO_2 (c-YSZ) substrates. These measurements

lead to experimental estimates of ν for (111) and (001) oriented films.

In_2O_3 thin films were grown on 1 × 1 cm YSZ substrates (PiKem, UK) in an ultrahigh-vacuum oxide molecular beam epitaxy (MBE) system (SVT, USA), as described in detail elsewhere.[13] Substrates were heated radiatively using a graphite filament. The substrates were cleaned by exposure to an oxygen atom beam at a substrate temperature of 900 °C. Growth runs on (111) oriented substrates were carried out with a substrate temperature of 700 °C for film thicknesses between 35 and 400 nm, while an ultrathin sample with a nominal average thickness of only 1 nm was grown on an (001) oriented substrate held at a temperature of 900 °C. The nominal growth rate was 0.035 nm s^{-1}, which was calibrated using the thickness from high-resolution transmission electron microscopy (HRTEM) measurements on the (111) samples. Atomic force microscopy (AFM) images showed that samples grew on (111) substrates essentially as continuous films. By contrast, the (001) sample adopted an island morphology[10,11,13,14] with a typical island thickness of about 5 nm, i.e., five times the thickness for a uniform film.

Diffraction measurements were conducted on two different synchrotron beamlines. The (111) samples were studied on the bending magnet beamline XMaS/BM28 at the European Synchrotron Radiation Facility (ESRF), Grenoble, France, using a photon energy of 12.398 keV, corresponding to a wavelength $\lambda = 1.0000$ Å. The (001) sample was studied on the undulator beamline I16 on the Diamond Synchrotron in the United Kingdom using 8.000 keV photons, corresponding to $\lambda = 1.5498$ Å. The diffractometers on these beamlines both allowed flexible access to reciprocal space using a simple point detector. Several reflections were studied for each sample, but here we confine attention to the off-axis (10 2 6) reflection for the (111) oriented sample and the (136) reflection for the (001) sample. The former is close to the allowed substrate (513) reflection, but the latter arises from superlattice ordering in the In_2O_3, and there is no substrate peak nearby. This absence enabled us to study the very weak scattering from the highly dilute (001) sample. Reciprocal space maps were constructed from a series of transverse scans, with stepping of the longitudinal wave-vector transfer between successive scans. The transverse wave-vector transfer was along the $[1\bar{1}0]$ direction for the (111) samples and along the [130] direction for the (001) sample. It should be noted that maps taken around the (006) reflection of the (001) sample with transverse wave vector along the [100] or [110] directions showed no evidence of splitting due to tilt in the epilayer, as has been observed for samples with nominal average thicknesses of 17 nm or greater.[14]

The reciprocal space maps for the (111) oriented samples are shown in Fig. 1 as plots of $Q[111]$ against $Q[1\bar{1}0]$: The dimensionless units in the plots are reciprocal lattice vectors of the substrate. In each map, the coordinates for unstrained In_2O_3 (assuming the bulk lattice parameter $a = 10.117$ Å) are shown as a circular dot. For the 35 nm sample (Fig. 1(a)) the maxima Q_I in the scattering from the epilayer are found at $Q_I[1\bar{1}0] = 2.8324$ and $Q_I[111] = 5.3590$, as indicated by the square dot. This is strongly displaced from $Q_0[1\bar{1}0] = 2.8765$ and $Q_0[111] = 5.2845$ for bulk In_2O_3. In plane, the epilayer comes close to matching the

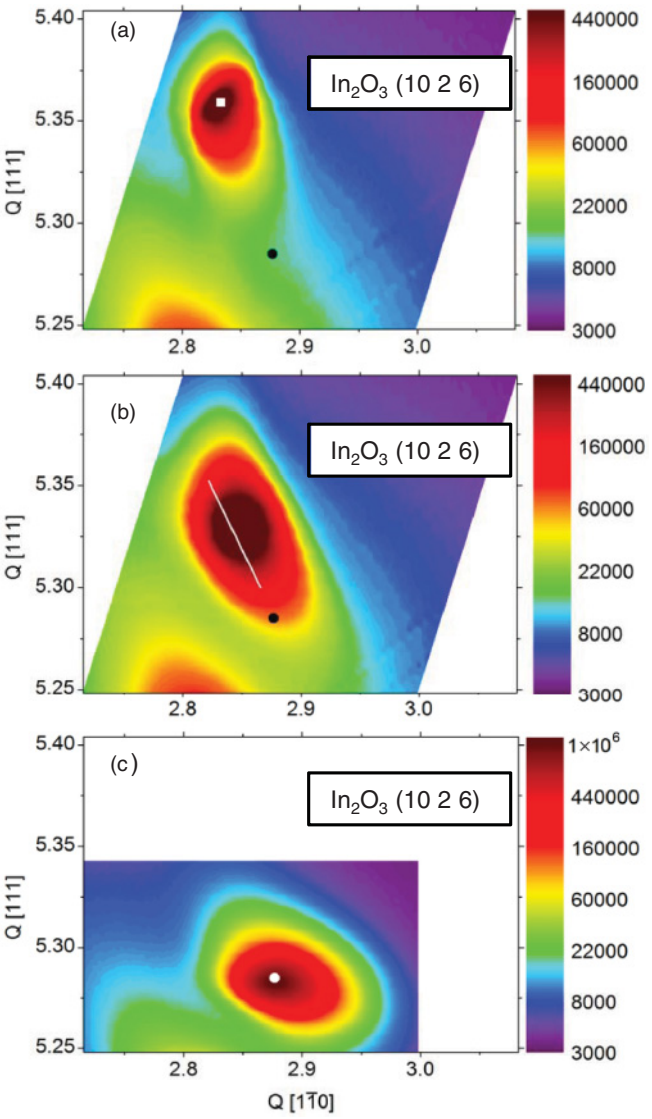

FIG. 1. (Color online) (a) Reciprocal space map for the (10 2 6) reflection of highly strained thin film of In_2O_3 grown on (111) oriented Y-stabilized ZrO_2 at 750 °C. The film thickness is estimated to be 35 nm. (b) Similar map for partially relaxed film with thickness of 105 nm. (c) Similar map for relaxed film with thickness of 420 nm. The longitudinal wave-vector transfer along the [111] direction and the transverse wave-vector transfer along the $[1\bar{1}0]$ direction are expressed in terms of reciprocal lattice units of the substrate. The circular spots mark the position of the (10 2 6) reflection for unstrained In_2O_3, while the square spot in (a) identifies the position of maximum intensity in the map. The line in panel (b) was derived from a linear least squares fit to a plot of $Q_I[111]^{-1}$ vs $Q_I[1\bar{1}0]^{-1}$, where the subscript I signifies the maximum in scattering intensity in successive transverse scans used to build up the map.

substrate, for which $Q[1\bar{1}0] = 2.8284$. Thus, the mismatch of 1.7% between substrate and epilayer is reduced to only 0.14% by in-plane strain. At the same time, there is a large increase in $Q[111]$ owing to the Poisson contraction normal to the surface. The globular shape of the contours indicates that there is little relaxation in the film. By contrast, for the 420 nm film [Fig. 1(c)], there is almost complete relaxation, and the coordinates for unstrained bulk In_2O_3 fall in the center

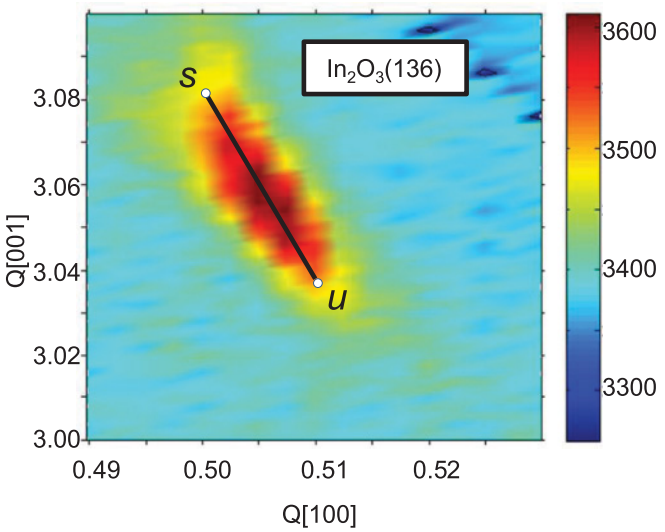

FIG. 2. (Color online) Reciprocal space map for (136) reflection of very thin film of In_2O_3 grown on (001) oriented Y-stabilized ZrO_2 at 900 °C. The average film thickness would be 1 nm for a layer-by-layer growth mode, but the film morphology is based on islands with a typical thickness of 5 nm. The longitudinal wave-vector transfer along the [001] direction and the [100] component of the transverse wave-vector transfer are expressed in terms of reciprocal lattice vectors of the substrate. The solid line links the two points s and u in the map used to derive a value for the Poisson ratio, where s denotes the limit where the epilayer is strained to match the substrate in plane.

of the contours that define scattering from the epilayer. For the intermediate 105 nm film, the reciprocal space map has an elongated ovoid shape: The principal axis slopes in a downward diagonal direction in the map, as indicated by the superimposed line. This map suggests a partially relaxed film structure: Close to the interface, the film is under tensile strain to bring the lateral periodicity toward that of the substrate, but strain is relaxed in moving away from the interface, and $Q[1\bar{1}0]$ moves up toward the value for bulk In_2O_3. In parallel with this variation, $Q[111]$ decreases as $Q[1\bar{1}0]$ increases owing to the Poisson effect, i.e., as tensile strain in the transverse direction is released, the compensating compressive strain in the longitudinal direction also decreases. The diagonal line in Fig. 1(b) extrapolates toward the reciprocal space coordinates for bulk In_2O_3. As shown in Fig. 2, a downward-sloping diagonal feature is also observed for the reciprocal space map for the (136) reflection of the (001) oriented sample, suggesting that there is also significant strain relaxation in the small thin islands that make up this sample.

The Poisson ratio is defined by the equation[16]

$$\frac{\varepsilon_\perp}{\varepsilon_\parallel} = \frac{(a^\perp - a_0^\perp)/a_0^\perp}{(a^\parallel - a_0^\parallel)/a_0^\parallel} = -\frac{2\nu}{1-\nu},$$

where $\varepsilon_\perp$ and $\varepsilon_\parallel$ are the strains normal and parallel to the surface; $a^\perp$ and $a^\parallel$ are the corresponding separations between atomic planes in the strained layer; and $a_0^\perp$ and $a_0^\parallel$ are the values for the unstrained system. We may write this relationship in terms of the reciprocal space coordinates for the (10 2 6) reflection of bulk In_2O_3 and for the position of maximum intensity in the map for the epilayer as

$$\frac{(Q_I[111])^{-1} - (Q_0[111])^{-1}}{(Q_I[1\bar{1}0])^{-1} - (Q_0[1\bar{1}0])^{-1}} \times \frac{3\sqrt{3}}{2\sqrt{2}} = -\frac{2\nu}{1-\nu},$$

where we have used the relationship

$$\frac{Q_0[111]}{Q_0[1\bar{1}0]} = \frac{3\sqrt{3}}{2\sqrt{2}},$$

and the reciprocal lattice coordinates are expressed in terms of reciprocal lattice vectors of the substrate. With this procedure, we obtain $\nu = 0.31 \pm 0.02$ for map 1 (a).

As mentioned already, with (001) oriented substrates, even the thinnest island films we have studied are not pseudomorphically strained, so it is not possible to adopt the previously outlined procedure to derive a value of the Poisson ratio. However, we can estimate the Q coordinates of the extremal points s and u in the map of Fig. 2 for the (136) reflection and hence write down:

$$\frac{(Q_s[001])^{-1} - (Q_u[001])^{-1}}{(Q_s[100])^{-1} - (Q_u[100])^{-1}} \times 6 = -\frac{2\nu}{1-\nu}.$$

With this approach, we obtain a somewhat lower value for the Poisson ratio of $\nu = 0.27 \pm 0.04$.

In principle, the "Poisson ratio" differs for samples subject to epitaxial strain in the (001) and (111) planes. In terms of elastic constants C_{ij}, we have for (001) oriented films:

$$\frac{2\nu(001)}{1-\nu(001)} = \frac{2C_{12}}{C_{11}},$$

while for (111) oriented films, there is the relationship[17]

$$\frac{2\nu(111)}{1-\nu(111)} = \frac{2C_{12} - 2C_0/3}{C_{11} + 2C_0/3},$$

where

$$C_0 = 2C_{44} - C_{11} + C_{12}.$$

Using the values of the elastic constants computed by Walsh *et al.* ($C_{11} = 297.75$ GPa, $C_{12} = 141.78$ GPa, and $C_{44} = 76.42$ GPa), the derived value for C_0 as defined above is only -3.13 GPa.[5,18] To two significant figures, one obtains $\nu(001) = 0.32$ and $\nu(111) = 0.33$. The calculated value of $\nu(111)$ is quite close to that of 0.31 found experimentally. In addition, $\nu(111) > \nu(001)$, which is also in agreement with experiment. However, the absolute experimental value of $\nu(001)$ is somewhat lower than expected from the calculated elastic constants.[19]

The present data may be compared with previous experimental work. Neerinck and Vink determined $\nu = 0.35$ from x-ray diffraction measurements on polycrystalline In_2O_3,[20] a value higher than found here. For structurally related Y-doped ZrO_2, Ingel *et al.* measured C_{11}, C_{12}, and C_{44} for single-crystal samples as a function of Y doping level using an acoustic wave pulse overlap technique and found that ν decreased from around 0.32 to around 0.30 as the Y_2O_3 fraction in $(Y_2O_3)_x(ZrO_2)_{1-x}$ doping level increased from 7 to 17%.[21] Selcuk and Atkinson inferred similar values by extrapolating data from measurements on polycrystalline samples of different densities back to zero porosity.[22] Thus, the current estimates are in line with values for a structurally related fluorite material.

In summary, the Poisson ratios of (111) and (001) oriented In_2O_3 epilayers were measured by synchrotron-based x-ray diffraction studies of strained thin films. The values obtained are in good agreement with those calculated by atomistic simulation procedures. There is therefore now a sound basis for using strain in ultrathin In_2O_3 films to tune the band gap of this increasingly important optoelectronic material.[5,23]

The Oxford molecular beam epitaxy (MBE) programme was supported under the Engineering and Physical Science Research Council (EPSRC) grant GR/S94148. KHLZ is grateful to Oxford University for the award of a Clarendon Scholarship. DJP is grateful to Christchurch Oxford for a Junior Research Fellowship. This work was supported by Royal Society Grant RG080399.

*Present address: Department of Chemistry, University College, London WC1H 0AJ, United Kingdom.
†Present address: Department of Materials, Imperial College London, Exhibition Road, London SW7 2AZ, United Kingdom.
‡Corresponding author:russell.egdell@chem.ox.ac.uk

[1] D. S. Ginley, H. Hosono, and D. C. Paine, Editors, *Handbook of Transparent Conductors* (Springer, New York, 2010).
[2] C. G. Granqvist, Int. J. Nanotech. **6**, 785 (2009).
[3] A. Walsh, J. L. F. Da Silva, S. H. Wei, C. Korber, A. Klein, L. F. J. Piper, A. DeMasi, K. E. Smith, G. Panaccione, P. Torelli, D. J. Payne, A. Bourlange, and R. G. Egdell, Phys. Rev. Lett. **100**, 167402 (2008).
[4] I. Hamberg, C. G. Granqvist, K. F. Berggren, B. E. Sernelius, and L. Engstrom, Phys. Rev. B **30**, 3240 (1984).
[5] A. Walsh, C. R. A. Catlow, K. H. L. Zhang, and R. G. Egdell, Phys. Rev. B **83**, 161202 (2011).
[6] M. Marezio, Acta Cryst. **20**, 723 (1966).
[7] K. H. L. Zhang, D. J. Payne, R. G. Palgrave, V. K. Lazarov, W. Chen, A. T. S. Wee, C. F. McConville, P. D. C. King, T. D. Veal, G. Panaccione, P. Lacovig, and R. G. Egdell, Chem. Mater. **21**, 4353 (2009).
[8] E. H. Morales, Y. B. He, M. Vinnichenko, B. Delley, and U. Diebold, New J. Phys. **10**, 125030 (2008).
[9] O. Bierwagen, and J. S. Speck, Appl. Phys. Lett. **97**, 072103 (2010).
[10] K. H. L. Zhang, A. Walsh, C. R. A. Catlow, V. K. Lazarov, and R. G. Egdell, Nano Lett. **10**, 3740 (2010).
[11] A. Bourlange, D. J. Payne, R. M. J. Jacobs, R. G. Egdell, J. S. Foord, A. Schertel, P. J. Dobson, and J. L. Hutchison, Chem. Mater. **20**, 4551 (2008).
[12] A. Bourlange, D. J. Payne, R. G. Egdell, J. S. Foord, P. P. Edwards, M. O. Jones, A. Schertel, P. J. Dobson, and J. L. Hutchison, Appl. Phys. Lett. **92**, 092117 (2008).
[13] A. Bourlange, D. J. Payne, R. G. Palgrave, J. S. Foord, R. G. Egdell, R. M. J. Jacobs, A. Schertel, J. L. Hutchison, and P. J. Dobson, Thin Solid Films **517**, 4286 (2009).
[14] R. A. Cowley, A. Bourlange, J. L. Hutchison, K. H. L. Zhang, A. M. Korsunsky, and R. G. Egdell, Phys. Rev. B **82**, 165312 (2010).
[15] A. Yamada, P. J. Fons, R. Hunger, K. Iwata, K. Matsubara, and S. Niki, Appl. Phys. Lett. **79**, 608 (2001).
[16] M. Birkholz, *Thin Film Analysis by X-ray Scattering* (Wiley-VCH, Weinheim, Germany, 2006).
[17] A. Segmuller, J. Vac. Sci. Technol. A **9**, 2477 (1991).
[18] A. Walsh, C. R. A. Catlow, A. A. Sokol, and S. M. Woodley, Chem. Mater. **21**, 4962 (2009).
[19] The value of $\nu(001)$ determined from the diagonal streak in reciprocal space is less reliable than $\nu(111)$ determined from the coherently strained (111) film owing to the very weak scattering from the (001) film. It should also be noted that the value of $\nu(111)$ determined from the map in Fig. 1(b) has an anomalously low value of 0.24.
[20] D. G. Neerinck, and T. J. Vink, Thin Solid Films **278**, 12 (1996).
[21] R. P. Ingel, and D. Lewis III, J. Am. Ceram. Soc. **71**, 265 (1988).
[22] A. Selcuk, and A. Atkinson, J. Eur. Ceram. Soc. **17**, 1523 (1997).
[23] K. H. L. Zhang, V. K. Lazarov, T. D. Veal, F. E. Oropeza, C. F. McConville, R. G. Egdell, and A. Walsh, J. Phys. Condens. Matter **23**, 334211 (2011).